HCC control by lycorine-based restraining of the MiR-224-5p/COLEC10 axis

Cai Chen, Junjie Zhao and Bo Qiu
Faculty of Medicine, Xinyang Vocational and Technical College, Xinyang, China

Abstract: Lycorine (LYC), as a natural alkaloid, possesses various significant biological activities. This study aims to investigate the impact and underlying mechanisms of LYC on the malignant progression of hepatocellular carcinoma (HCC). The levels of miR-224-5p, collectin subfamily member 10 (COLEC10) and inflammatory factors were quantified by RT-qPCR. The levels of COLEC10 and EMT relevant proteins were identified by Western blotting. Effects of LYC on the biological behaviors of HCC cells were assessed. The Dual-Luciferase reporter assay was used to verify the targeting relationship between miR-224-5p and COLEC10. Additionally, A subcutaneous xenograft model of HCC was created in nude mice. HCC tissues and cells exhibited elevated level of miR-224-5p, while COLEC10 was lower. Overexpression miR-224-5p enhanced HCC cells proliferation, migration, invasion, EMT and inflammatory response, while suppressed apoptosis. Moreover, miR-224-5p targeted the expression of COLEC10 negatively. COLEC10 silenced could offset the suppression of HCC advancement induced by silenced miR-224-5p. While LYC down regulated miR-224-5p level and inhibited the HCC malignant progression. In conclusion, LYC can down regulate the levels of miR-224-5p, upregulate the levels of COLEC10 and thus inhibit the malignant progression of HCC.

Keywords: hepatocellular carcinoma, Lycorine, miR-224-5p, Collectin subfamily member 10, proliferation

INTRODUCTION

Occupying ninety percent of all primary liver cancer cases, hepatocellular carcinoma (HCC) is recognized as the fifth most widespread malignancy globally; it ranked second in the causes of cancer-associated fatalities, significantly impacting human health (Nagaraju *et al.*, 2022, Wen *et al.*, 2022). Statistics show that for HCC patients in Asian countries, their survival rate within five years is merely 18% (Hassanipour *et al.*, 2020). If diagnosed early, HCC patients can receive treatment with local ablation, liver transplantation and surgical resection methods (Hartke *et al.*, 2017, Foglia *et al.*, 2023); whereas, most HCC patients in their first diagnosis have progressed to the middle and even late stages, making tumor excision infeasible. Hence, the overall cure rate and survival rate of HCC are low (Chedid *et al.*, 2017, Ayuso *et al.*, 2018). This situation highlights the call for novel and efficient drugs to retard the advance of HCC.

As a natural alkaloid acquired from the family of Amaryllidaceae, Lycorine (LYC) is active in resisting inflammation, tumors, viruses and so on (Roy *et al.*, 2018, Di Sotto *et al.*, 2023). As proved by Sun *et al*., LYC can refrain the expansion of breast cancer cells, intercept the G2/M phase of cell cycle, stimulate apoptosis and suppress Epithelial-mesenchymal transition (EMT) (Sun *et al.*, 2023). Additionally, LYC can refrain the expression of inflammatory cytokines and ameliorate rat liver fibrosis based on its dosage (Alkreathy *et al.*, 2022).

_____
Corresponding authors: e-mails: diru00914@163.com

Yet, no literature mentioned LYC's intervention in the malignant evolution of HCC.

microRNA (miRNA) acts as a gene expression regulator as it can attach directly to mRNA, inhibiting mRNA translation, or degrade the target mRNA (Li *et al.*, 2020). As demonstrated in considerable articles, the evolution of HCC is primarily controlled by miRNA that regulates various oncogenes and tumor-inhibiting factors; changing miRNA's expression degree may interfere with malignant biological behaviors in cells (Sartorius *et al.*, 2018, Oura *et al.*, 2020). Furthermore, miR-224-5p in HCC cells exists at a higher level than that in normal tissues, thus can be used creatively for diagnosing HCC in the early stage (Zhang *et al.*, 2017).

Against this background, the study firstly surveyed the LYC's interference with HCC cells' viability and miR-224-5p's expression. Next, an exploration was made on the interference of over-expressed miR-224-5p with the destructive biological attributes of HCC and the expressions of inflammatory cytokines including interferon-γ (IFN-γ), interleukin-2 (IL-2), tumor necrosis factor-α (TNF-α) and interleukin-1β (IL-1β) in HCC cells. By database screening, collectin subfamily member 10 (COLEC10) was affirmed as a target gene in the downstream of miR-224-5p. Further, miR-224-5p and COLEC10 were silenced respectively for exploring their influences on the aggressive evolution of HCC. Finally, the impacts of LYC treatment on HCC growth in nude mice were investigated, aiming at contributing to the early HCC diagnosis and treatment.

Survey methodology and materials
Sampling of clinical tissues
A total of 60 HCC patients treated at Faculty of Medicine, Xinyang Vocational and Technical College provided the tissue samples used in this survey. The tissue samples were collected from their cancerous and neighboring non-cancerous tissues and then cleaned and immersed in liquid nitrogen before use. This survey was conducted under the permission of the Ethics Board of Faculty of Medicine, Xinyang Vocational and Technical College and the informed consent for the use of samples signed by all the participants (HK-202303-A). 33 cases of male patients and 27 cases female patients, age range 39-59 years [mean age (52.50±8.51) years, 95% confidence intervals (CI): 50.3, 54.7]. The criteria for the selection of HCC patients were: (1) patients with pathologically confirmed HCC; (2) age ≥18 years, gender unrestricted; (3) complete personal information of the patients; (4) provision of a signed informed consent form. The exclusion criteria for patients were: (1) those who had received treatment (including but not limited to radiotherapy, chemotherapy, targeted therapy, or immunotherapy, etc.); (2) pathological diagnosis of benign tumor; (3) history of other malignant tumors; (4) presence of extrahepatic metastasis.

Cultivation and transfection of cells
The HCC cell lines (Hep3B, Huh-7, MHCC97, SMMC-7721, and HepG2) and normal human liver cells (LO-2) were all obtained from the Shanghai Cell Bank of the Chinese Academy of Sciences. The cells were cultivated in DMEM (source: Gibco, Grand Island, NY, USA) mixed with 1% of penicillin and streptomycin (Gibco) and 10% of fetal bovine serum (Gibco) with the cultivation temperature at 37°C and the cultivation condition containning 5% CO_2. The cells got passaged once three days and the culture medium was replaced at an interval of two days. By virtue of Lipofectamine 3000 (Invitrogen, Carlsbad, CA, USA), MHCC97 and SMMC-7721 were transfected by such miR-224-5p mimics (mimics), miR-224-5p inhibitor (inhibitor), shRNA-COLEC10, or negative controls (mimics-NC, inhibitor-NC, and shRNA-NC) as synthesized by Sangon Biotech (Shanghai, China) respectively (Hu *et al*., 2023).

RT-qPCR-based assays
The tissues and cells were treated using Trizol reagent (Invitrogen) to collect the total RNA. Then the total RNA was transcribed reversely to cDNA by applying the AMV reverse transcriptase produced by Sigma-Aldrich, St. Louis, MO, USA. Subsequently, the SYBR Green qPCR mix kit prepared by TAKARA, Tokyo, Japan was applied for PCR amplification (Wang *et al*., 2021). In this assay, GAPDH was as the internal control and the primers with the following sequences:

miR-224-5p: Forward: 5'-GGCTTTGTAGTCACTAGGG

CA-3', Reverse: 5'-TCAAGTCACTAGTGGTTCCGT-3'.
U6: Forward: 5'-CCCTTCGGGGACATCCGATA-3', Reverse: 5'-TTTGTGCGTGTCATCCTTGC-3'.
COLEC10: Forward: 5'-TTTCGGGGAGTTCGCAAT CA-3', Reverse: 5'-GGGTCCCCTCTCCTGATTCT-3'.
GAPDH: Forward: 5'-ATGTTGCAACCGGGAAGGAA-3', Reverse: 5'-CGCCCAATACGACCAAATCAGA-3'.
IFN-γ: Forward: 5'-CAGCTCTGCATCGTTTTGGG-3', Reverse: 5'-CTGTTTTAGCTGCTGGCGAC-3'.
IL-2: Forward: 5'-TCCCAAACTCACCAGGATGC-3', Reverse: 5'-AGAGCCCCTAGGGCTTACAA-3'.
IL-1β: Forward: 5'-GGGGCGTCCTTCATATGTGT-3', Reverse: 5'-GGCAGCTCCTGTCTTGTAGG-3'.
TNF-α: Forward: 5'-GAGACAGATGTGGGGTGTGAG-3', Reverse: 5'-TCCTAGCCCTCCAAGTTCCA-3'.

CCK-8-based assays
MHCC97 and SMMC-7721 in the log phase were accommodated in a 96-well plate, with $2.0×10^4$ cells per well. After attaching to the well wall, the cells were rid of the original culture medium and incubated with different doses of LYC for 24 hours. Then, each well was distributed with 100μL of complete culture medium mixed with 10% of CCK-8 reagent (Beyotime, Shanghai, China). Afterward, the plate was put in an incubator (37°C) for 2 hours of cultivation. Finally, the OD_{450} values of the cells were examined by using a microplate reader (Thermo Fisher Scientific, Waltham, MA, USA) (Li *et al*., 2021).

Scratch healing assays
6-well cell culture plate was marked with horizontal lines in advance and then dosed with MHCC97 and SMMC-7721 cells in log phase. After the cells attached to the well wall, a sterile pipette tip (20μL) was employed to gently draw a line vertical to the marked horizontal lines at the bottom of the plate. Next, the cells were cleaned twice using PBS and then added with serum-excluding DMEM medium for incubation in an incubator. The scratch healing status was observed at 0 and 24 hours respectively. The width of the scratch was analyzed and measured using the Image J software (Li *et al*., 2021).

Transwell-based assays
Matrigel gel (Sigma-Aldrich) was diluted to 1:6 by a serum-excluding DMEM medium and each trans well chamber (Corning, Tewksbury, MA, USA) was administered with 100μL of the diluted gel and incubated for one night in an incubator. On the next day, the liquid remained in the chamber was sucked and serum-excluding DMEM medium was dosed in the chamber to hydrate the substrate. 200μL of the cell suspension was dosed to the upper chamber, alongside an appropriate amount of DMEM medium mixed with 10% of fetal bovine serum to the lower chamber, staying for 36 hours of culture. After that, the matrix gel and the cells in the upper chamber were washed away; the remained cells

1094

Pak. J. Pharm. Sci., Vol.37, No.5, September-October 2024, pp.1093-1105

were fixed for 30 minutes by adding 4% paraformaldehyde (Solarbio, Beijing, China) and dyed with 0.1% crystal violet for 5 minutes (Sigma-Aldrich), and then rinsed for two repetitions using PBS solution. Microscope was applied to observe each well from five fields randomly selected and took the pictures, followed by counting the number of invaded cells. Except that Matrigel was not dosed in the upper chamber, the migration assay followed the steps of the invasion assay (Wang *et al.*, 2022).

Flow Cytometry-based Assays

Log-phase MHCC97 and SMMC-7721 cells were washed by PBS solution twice and added with 500μL binding buffer involving 5μL Annexin-V-FITC (HY-K1073; Med Chem Express, Monmouth Junction, NJ, USA) and 5μL propidium iodide (Beyotime) and blended gently, staying for 15 minutes avoiding light at the room temperature. Then the samples were transferred to the sample tubes specialized for flow cytometry. The cell apoptosis was examined within 1 hour using a flow cytometer (Wang *et al.*, 2022).

Western blot-based assays

Cell lysates were prepared using RIPA lysis buffer (Solarbio) to extract proteins, and the protein concentrations were tested by the BCA assay kit (Beyotime). After processing by gel electrophoresis, the samples were transferred to PVDF membrane (Invitrogen), along with 1 hour of blocking. After washing, the membrane was put in a solution of primary antibody against E-cadherin (ab231303; Abcam; diluted to 1:1000), primary antibody against N-cadherin (ab18203; Abcam; diluted to 1:1000), or primary antibody against COLEC10 (PA5-122077; Invitrogen; diluted to 1:1000) for one night of incubation in a setting of 4°C. The following day, the membrane was rinsed thrice and then incubated for 1.5 hours with goat anti-rabbit secondary antibody IgG (31460; Invitrogen; diluted to 1:10000). Then, the membrane was rinsed for another three repetitions, ECL luminescent solution (Med Chem Express, Monmouth Junction, NJ, USA) was added to cover the entire membrane, gel imaging system (WD-9413B, Beijing Liuyi Biotechnology Co., Ltd, Beijing, China) was used to develop and scan the image. The grayscale values of the images were assessed by the Image J software. GAPDH (MA1-16757; Invitrogen; diluted to 1:1000) served as the internal control (Li and Jiang, 2020).

Dual-luciferase reporter assays

Sangon Biotech synthesized and provided the 3′UTR wild-type (WT) and mutant-type (MUT) nucleotide sequences of COLEC10 containing the site for binding to miR-224-5p. By virtue of Lipofectamine 3000, the MHCC97 and SMMC-7721 cells were co-transfected by COLEC10-WT & mimics-NC, COLEC10-WT & mimics, COLEC10-MUT & mimics-NC and COLEC10-MUT & mimics separately. Following 48 hours of incubation, the cells were collected and examined by Dual-luciferase assay kits (Solarbio) to acquire the luciferase activity in the cells (Wang *et al.*, 2023).

Subcutaneous tumor in nude mice

4~6-week-old male BALB/c nude mice (15-20g) were purchased from Beijing Vital River Laboratory Animal Technology Co., Ltd. (Beijing, China). They were housed in a clean-grade animal facility with room temperature of 22.5~28°C, relative humidity of 45%~55% and 12-hour light/12-hour dark cycle, with free access to food and water. The nude mice were splitted into two groups. Each group contained 6 mice. Each nude mouse received 0.2 mL (1×10^7 cells/mL) of log-phase MHCC97 cell suspension by hypodermic injection (Wang *et al.*, 2022). On days 0, 7 and 14 after 24 hours post inoculation, the nude mice were injected with 100μL of LYC (5 mg/kg) or PBS through the tail vein. The survival statuses of the mice were monitored and a caliper was utilized to measure the formed subcutaneous tumors on days 7, 14, and 21 in turn. On day 21, the mice were euthanized post anesthesia; the tumors were taken out and photographed for documentation. All experimental operations were approved by Ethics Committee (ethics approval No.: 20229K113) and comply with the ethical code for experimental animals.

STATISTICAL ANALYSIS

Each assay was conducted three times for the minimum. The outcomes are presented as the average value ± standard deviation. The Prism (Graphpad 9.0) was used for plotting. SPSS 26.0 was employed for variance analysis and student's t-tests. "*", "#" and "&" denote significant variances from the respective control groups (P<0.05).

Survey results

miR-224-5p's Expression in HCC Cells and LYC's Impact on HCC Cells
As detected by RT-qPCR, miR-224-5p contents in HCC tissues (1.42±0.39, 95%CI: 1.1136, 1.7340) significantly surpassed those in neighboring tissues (0.58±0.24, 95% CI: 0.3623, 0.7529), P<0.05 (fig. 1A-1B). The Kaplan-Meier plotter (http://kmplot.com/analysis/) based analysis results show that HCC patients with excessively-expressed miR-224-5p had poor survival rate (fig. 1C). Besides, miR-224-5p's contents were found at a low level in normal human liver cells (LO-2) but heightened HCC cell lines (for example, Huh-7, Hep3B, MHCC97, SMMC-7721 and HepG2), especially in the cell lines numbered MHCC97 and SMMC-7721, P<0.05 (fig. 1D). Consequently, MHCC97 and SMMC-7721 cells were selected and involved in the subsequent assays.
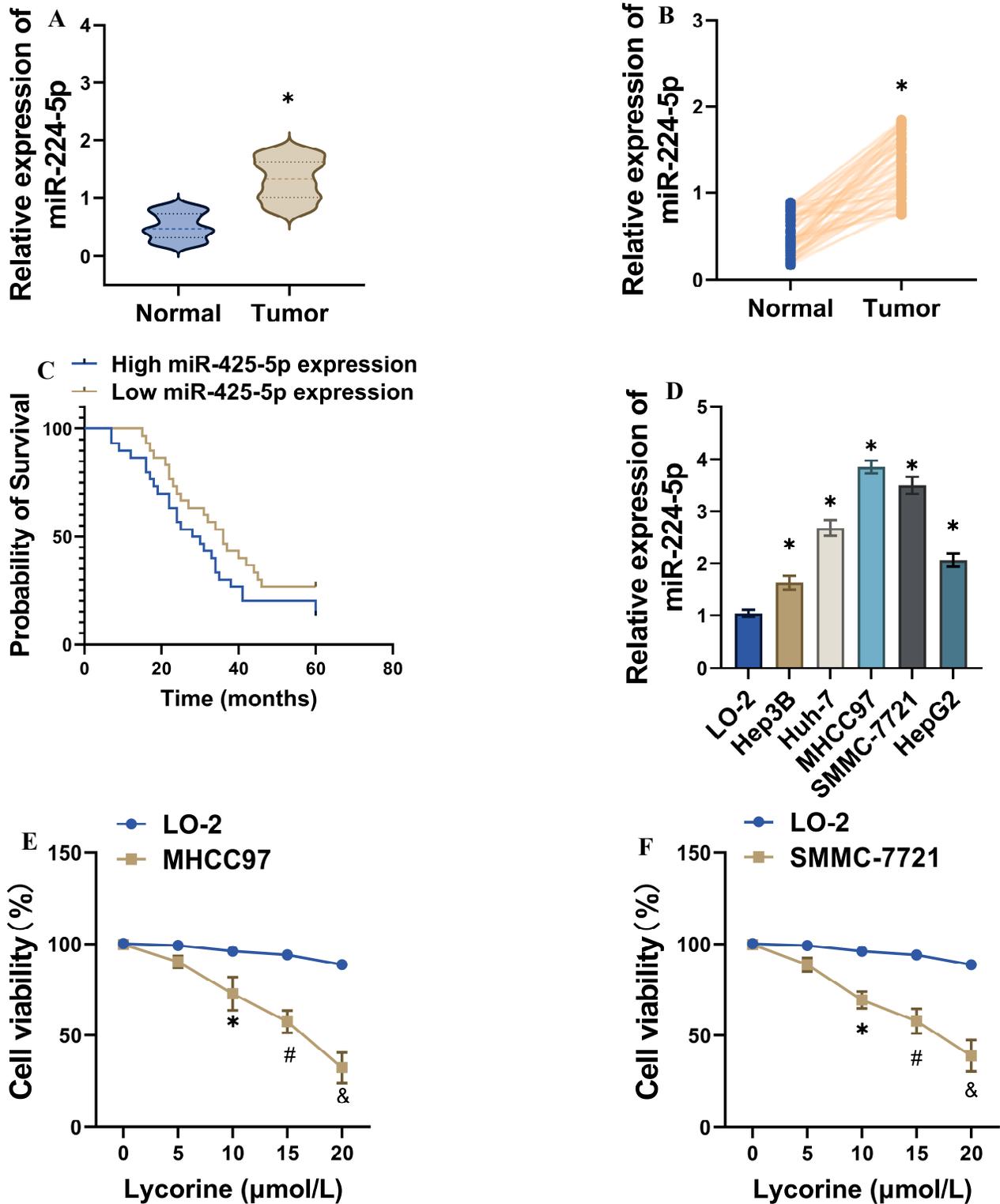
(A-B) miR-224-5p's expression in HCC tissues and the tissues adjacent to the cancer

(C) The relation between miR-224-5p expression and HCC prognosis

(D) miR-224-5p's expression in diverse cells detected by RT-qPCR assay

(E-F) LYC's impacts on the activity of MHCC97 and SMMC-7721 cells assessed by CCK-8 assays

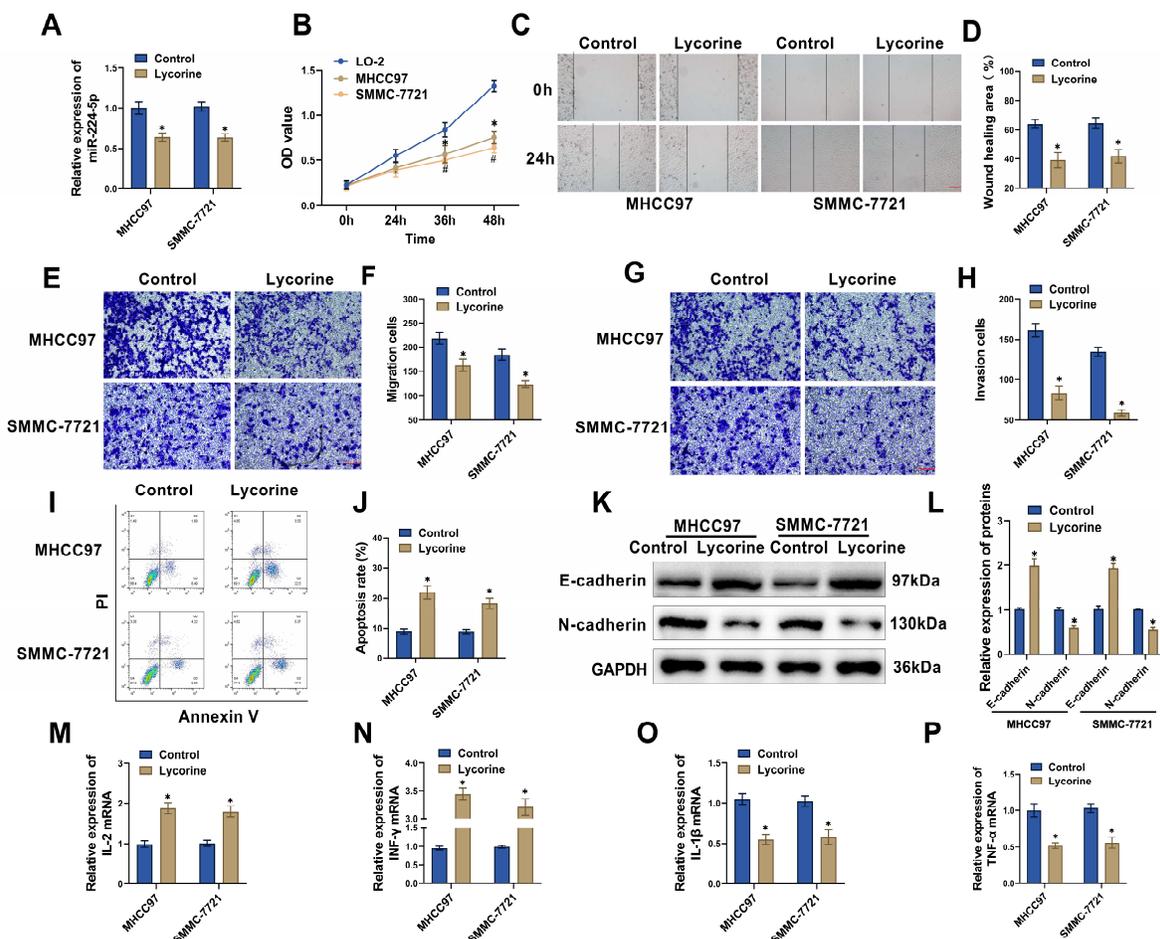**Fig. 1**: miR-224-5p's expression in HCC cells and LYC's impact on HCC cells

(A) miR-224-5p's expression in diverse cells as found through RT-qPCR assays
(B) The expansion of HCC cells as found through CCK-8 assays
(C-D) The movement of HCC cells as found through scratch healing assays
(E-H) The numbers of moved and invaded HCC cells as detected by transwell assays
(I-J) The rate of HCC cell apoptosis as detected by flow cytometry
(K-L) The protein levels of N-cadherin and E-cadherin detected by Western blotting
(M-P) The expressed contents of IL-2, INF-γ, IL-1β and TNF-α detected by RT-qPCR assays

Fig. 2: LYC's impact on HCC cells' biological performance

By detecting the influences of different doses of LYC on cell viability with the CCK-8 method, it was uncovered that LYC at the doses of 10, 15 and 20μmol/L could dampen the viability of MHCC97 and SMMC-7721 cells to a great extent, P<0.05, but brought no large effect to the activity of LO-2 cells, P>0.05 (fig. 1E-1F). In the following assays, the dose of LYC at 15μmol/L was applied.

***LYC's Impact on HCC cells' biological performance***
RT-qPCR result showed that the MHCC97 and SMMC-7721 cells, after being treated with LYC, <u>had</u> evidently dampened miR-224-5p levels, P<0.05 (fig. 2A). The proliferation of cells were tested with CCK-8. As a result, LYC restrained the expansion of MHCC97 and SMMC-7721 cells within 48 hours, P<0.05 (fig. 2B). The outcomes from scratch healing assay implied that the said

two types of cells treated with LYC acquired greatly lowered ability to migrate, P<0.05 (fig. 2C-2D). Further, transwell assay was conducted for testing the cell movement and penetration. The results showed that following LYC treatment, the MHCC97 and SMMC-7721 cells moved and penetrated less, P<0.05 (fig. 2E-2H). By detection with Flow cytometry method, the MHCC97 and SMMC-7721 cells were found at an elevated apoptotic rate post LYC treatment, P<0.05 (fig. 2I-2J). Over Western blot assay post LYC treatment, the said two cell lines were monitored acquiring heightened E-cadherin contents but lessened N-cadherin contents. This data denoted that LYC retarded the EMT of HCC cells, P<0.05 (fig. 2K-2L). Moreover, following LYC administration, the two cell line displayed highly raised contents of IL-2 and INF-γ but excessively lowered the IL-1β and TNF-α contents, P<0.05 (fig. 2M-2P).
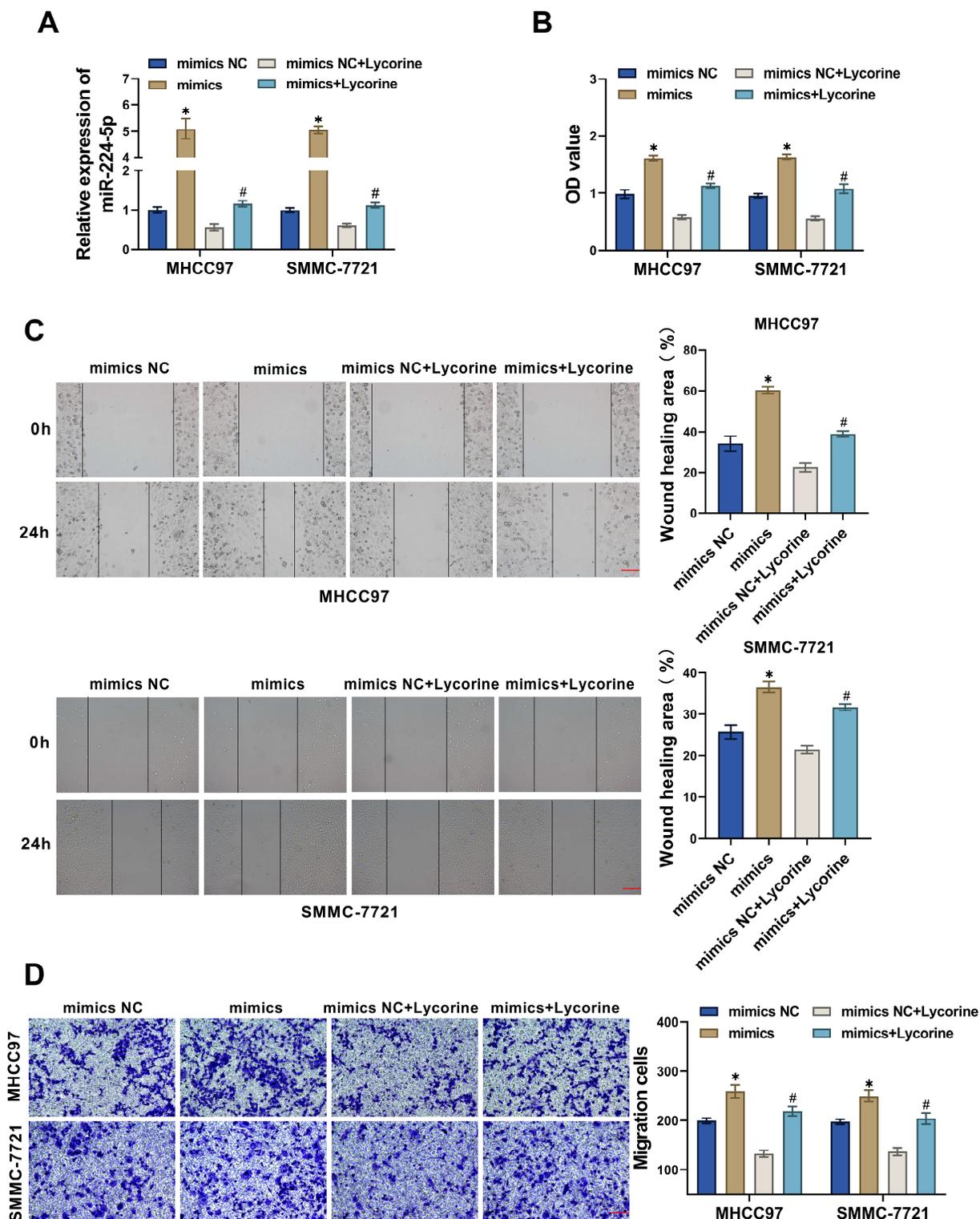
(A) miR-224-5p's expression in diverse cells as found by RT-qPCR assay
(B) The expansion of HCC cells found by CCK-8 assay
(C) The movement of HCC cells found by scratch healing assay
(D) The numbers of migrated and invasived HCC cells detected by transwell assay

Fig. 3: LYC-based suppression of HCC cell expansion and movement by retarding the expression of miR-224-5p
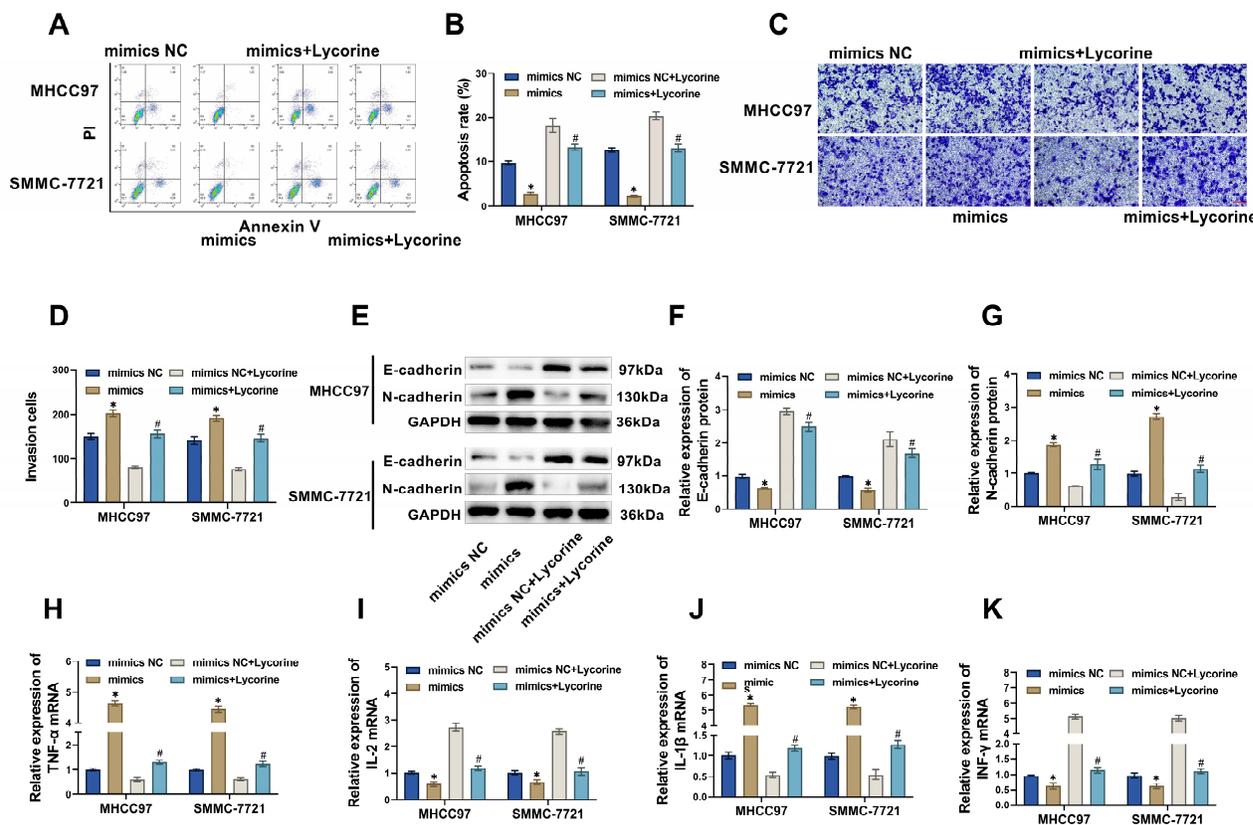
(A) The rate of HCC cell apoptosis detected by flow cytometry
(B) The expansion of HCC cells found by CCK-8 assays
(C-D) The numbers of invaded HCC cells detected by transwell assays
(E-G) The protein levels of N-cadherin and E-cadherin assessed by Western blotting
(H-K) The expressed contents of IL-2, INF-γ, IL-1β and TNF-α detected by RT-qPCR assays

Fig. 4: LYC-based promotion of HCC cell apoptosis and restraining of cell movement by silencing miR-224-5p

LYC-based suppression of hcc cell expansion and movement by retarding the miR-224-5p expression

As detected with the RT-qPCR, miR-224-5p expression became intensified after the cells got transfected with mimics but dampened with the administration of LYC, P<0.05 (fig. 3A). Notably, LYC restrained the viability of MHCC97 and SMMC-7721 cells; however, this restraining extent was partially offset following the transfection with mimics, P<0.05 (fig. 3B). The scratch healing assay consequences indicate that LYC treatment could alleviate the movement of MHCC97 and SMMC-7721 cells, whereas this alleviation could be counteracted somewhat by heightening miR-224-5p levels, P<0.05 (fig. 3C). The transwell assays also proved that LYC could lessen the number of moved cells, while expressing miR-224-5p over much could recover the cells' movement ability partially, P<0.05 (fig. 3D). All these consequences demonstrated that LYC inhibited the expansion and movement of MHCC97 and SMMC-7721 cells by lowering the miR-224-5p level.

LYC-based promotion of HCC cell apoptosis and Restraining of cell movement by silencing miR-224-5p

The cell apoptosis status evaluated by Flow cytometry denotes that MHCC97 and SMMC-7721 cells treated with LYC suffered from intensified apoptosis, while this intensification was eased following miR-224-5p's excessive expression, P<0.05 (fig. 4A-4B). The transwell assays demonstrated that the cells dosed with LYC became less invasive; yet, this phenomenon was reversed partially by expressing miR-224-5p highly, P<0.05 (fig. 4C-4D). As observed through the Western blot assays, MHCC97 and SMMC-7721 cells experienced a large decline in N-cadherin contents while a large rise in E-cadherin contents following the dosing of LYC. These data imply that LYC prevented HCC cells from EMT, while the excessively heightened miR-224-5p expression alleviated this prevention effect, P<0.05 (fig. 4E-4G). Furthermore, after LYC administration, the two lines of HCC cells witnessed remarkable elevation in IL-2 and INF-γ contents and reduction in TNF-α and IL-1β contents, which however was retarded with the heightening of miR-224-5p levels, P<0.05 (fig. 4H-4K).
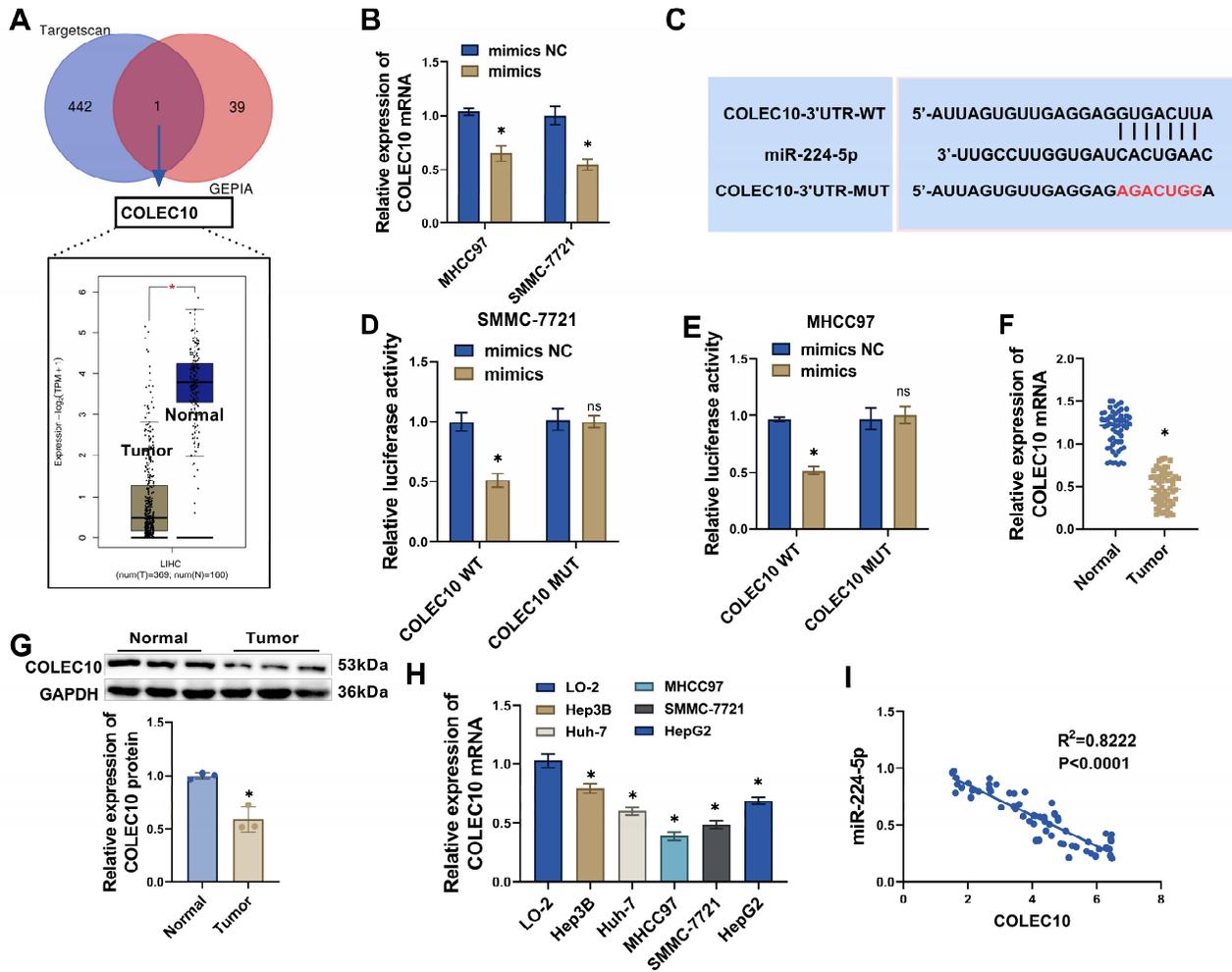
(A) Screening of COLEC10 and the expression of COLEC10 in HCC cells
(B) The expression of COLEC10 in different tissues was assessed by RT-qPCR assay
(C) The binding sequences between miR-224-5p and COLEC10
(D-E) The targeting connection between miR-224-5p and COLEC10 validated through Dual-Luciferase reporter assay
(F-G) The expressed content of COLEC10 in diverse tissues
(H) The expressed level of COLEC10 mRNA in diverse cells as monitored by RT-qPCR assay
(I) The linear relationship between miR-224-5p and COLEC10

Fig. 5: Screening the target gene of miR-224-5p

Above all, LYC contributed to the apoptosis of HCC cells and weakened the penetration, EMT, and inflammation of such cells by dampening miR-224-5p's expression.

Screening the Target Gene of miR-224-5p
Based on GEPIA (http://gepia.cancer-pku.cn/) and Target Scan Human 8.0 (https://www.targetscan.org/vert_80/) databases, COLEC10 was evaluated and confirmed as a target gene in the downstream of miR-224-5p. According to the GEPIA database, COLEC1 contents in HCC tissues were inferior to those in normal tissues much, $P<0.05$ (fig. 5A). Following miR-224-5p's over expression, the expressed COLEC10 mRNA levels reached a significantly low leve, $P<0.05$l (fig. 5B). Fig. 5C

illustrates the speculated site for miR-224-5p to attach to the COLEC10-3′UTR-WT. Results from the dual-luciferase reporter assays display that miR-224-5p when expressed over high could greatly impede the luciferase signal of COLEC10 WT, $P<0.05$, but had no apparent effect on COLEC10 MUT, $P>0.05$ (fig. 5D-5E). The expression of COLEC10 detected by Western blot and RT-qPCR assays aligned with that recorded in the GEPIA database: namely, the COLEC10 expression was at a lowered level in HCC tissues and cells, $P<0.05$ (fig. 5F-5H). Meanwhile, the expression of COLEC10 was under negative control by miR-224-5p in a targeted way, as presented in the linear regression relationship between miR-224-5p and COLEC10 levels (fig. 5I).
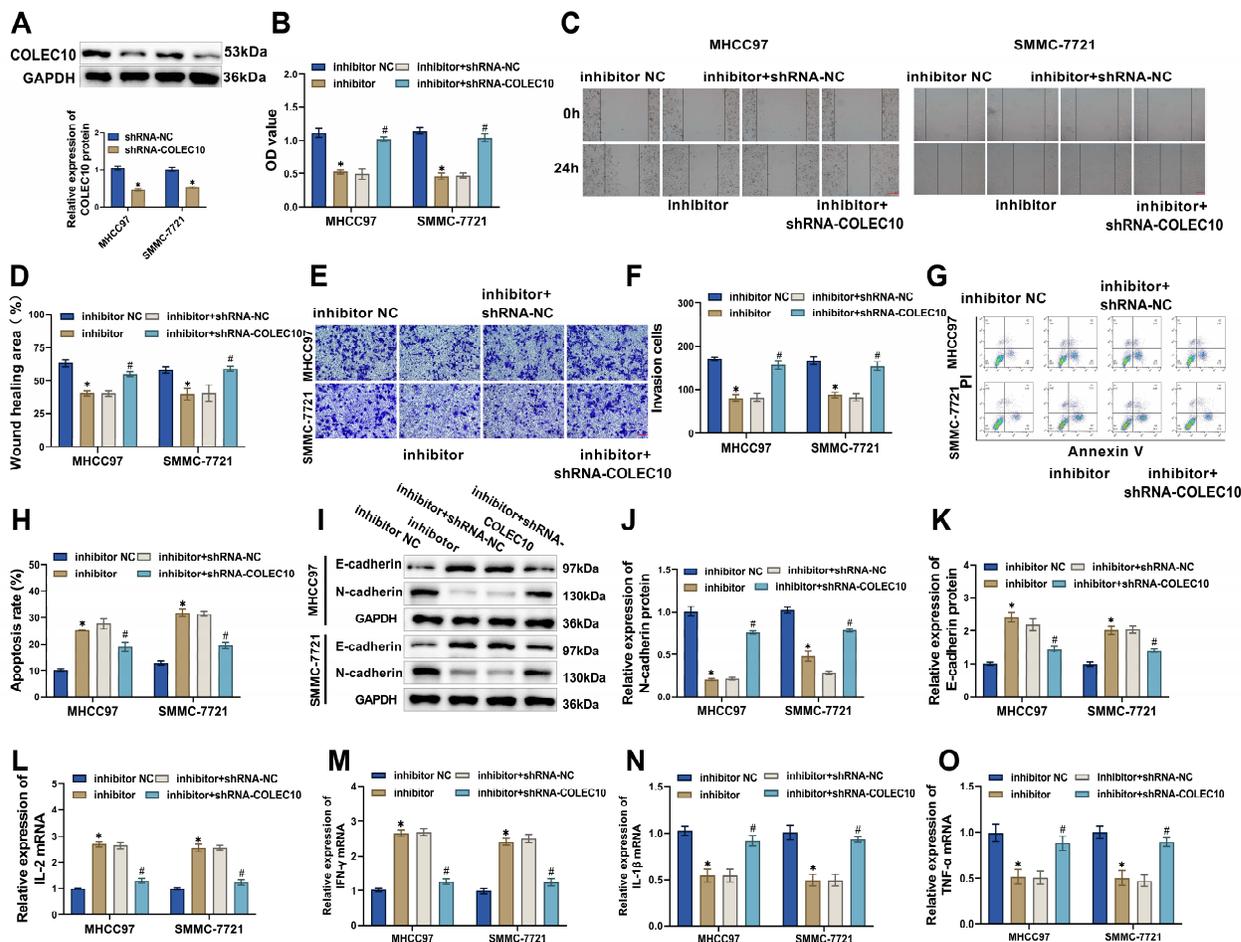
(A) The protein level of COLEC10 was examined by Western blot assay
(B) The expansion of HCC cells was detected by CCK-8 assay
(C-D) The movement of HCC cells was assessed by scratch healing assay
(E-F) The numbers of invaded HCC cells were detected by transwell assays
(G-H) The rate of HCC cell apoptosis was detected by Flow cytometry
(I-K) The protein levels of N-cadherin and E-cadherin were assessed with Western blot method
(L-O) The expressed contents of IL-2, INF-γ, IL-1β and TNF-α mRNA detected by RT-qPCR assay

Fig. 6: The effect of silencing COLEC10 in partially counteracting the HCC advancement suppressed by dampening the miR-224-5p expression

The Effect of Silencing COLEC10 in Partially Counteracting the HCC Advancement Suppressed by Dampening the miR-224-5p Expression

After transfecting MHCC97 and SMMC-7721 cells with shRNA-COLEC10, the silencing efficiency of COLEC10 was tested with the Western blot method. The result indicated a highly lowered contents of COLEC10 protein, $P<0.05$ (fig. 6A). Results from the subsequent CCK-8 assays disclose that silencing miR-224-5p largely weakened the viability of MHCC97 and SMMC-7721 cells, while silencing COLEC10 partially reversed this decrease in the cell viability, $P<0.05$ (fig. 6B). Outcomes from the scratch healing assays and transwell assays reveal that the MHCC97 and SMMC-7721 cells became less movable and invasive after miR-224-5p silencing but was recovered partially with the diminishing of COLEC10, $P<0.05$ (fig. 6C-6F); MHCC97 and SMMC-7721 cells' apoptosis became intensified following the dampening of miR-224-5p, which trend however was weakened partially with the lowering of COLEC10 levels, $P<0.05$ (fig. 6G-6H). In the MHCC97 and SMMC-7721 cells with silenced miR-224-5p, E-cadherin was assessed at a greatly raised level, while E-cadherin was at a clearly reduced level, hence the EMT was inhibited. With the retarding of COLEC10 expression, the EMT inhibited for that reason became restored to some extent, $P<0.05$ (fig. 6I-6K). In the meantime, the HCC cells with silenced miR-224-5p presented highly enhanced expressions of IL-2 and INF-γ and largely dampened expressions of TNF-α and IL-1β; this consequence was overturned partially after COLEC10 was diminished, $P<0.05$ (fig. 6L-6O).

A

B

C

D
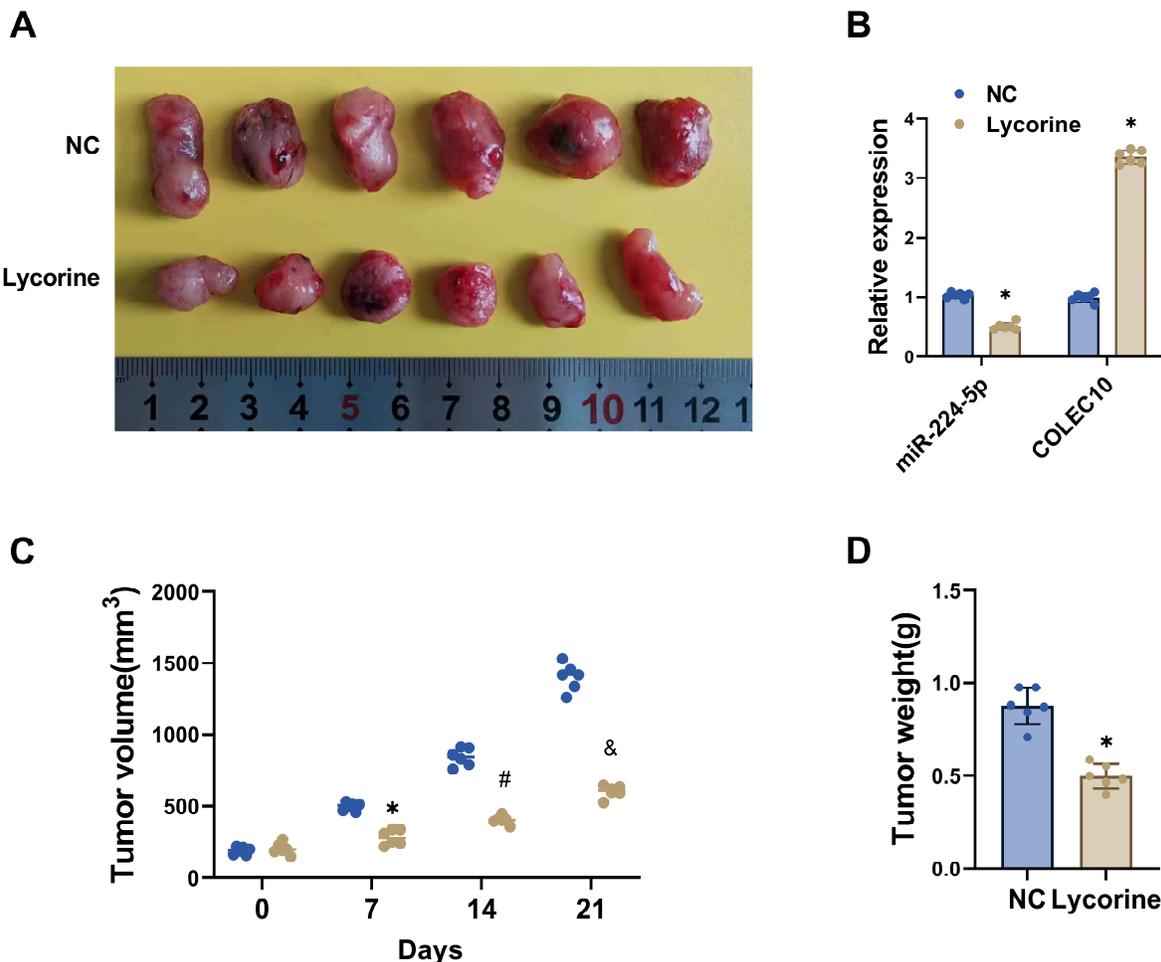
Experiment in vivo

HCC subcutaneous tumor models were formed in nude mice. As depicted in the tumor picture (fig. 7A), the LYC-treated group exhibited smaller HCC tumor volumes, $P<0.05$. With the RT-qPCR method, the intervention of LYC in the expressions of miR-224-5p and COLEC10 were tested in the mice. As the outcomes of LYC treatment, the miR-224-5p expression was dampened significantly, whereas the COLEC10 expression got amplified, $P<0.05$ (fig. 7B); tumors in the nude mice became shrunk and lightened, $P<0.05$ (fig. 7C-7D). These outcomes verified that LYC could hold up the growth of HCC tumor.

DISCUSSION

A primary active element of Amaryllidaceae, LYC, has been shown to hinder the advancement of multiple malignancies, for instance, polymorphic glioblastoma, cervical cancer, and rectal cancer (Shen *et al.*, 2018, Hu *et al.*, 2020, Li *et al.*, 2022). According to the research by Zhai *et al.*, LYC (5-50 μM) has no effect on the viability of human normal breast epithelial cells (MCF-10A cells), but it can significantly reduce the viability of breast cancer cells (MCF7 and T47D cells) (Zhai *et al.*, 2023). In this work, CCK-8 assay showed that LYC refrained the activity of MHCC97 and SMMC-7721 cells in proportion to the LYC dose, but posed no effect on the activity of normal liver cells. LYC inhibited the multiplication, movement and penetration of HCC cells and induced apoptosis. As further demonstrated by the subcutaneous xenograft tumor models formed in nude mice, LYC treatment significantly suppressed the growth of HCC tumors. Likewise, as observed by Yu *et al.*, LYC stimulated the apoptosis and autophagy in HCC cells, significantly inhibiting *in vitro* and *in vivo* multiplication of HCC cells (Yu *et al.*, 2017).

As endogenous regulators of gene expression, miRNAs participate in the immunologic process of tumors and are pivotal in the tumor occurrence and advance (He *et al.*, 2020, Diener *et al.*, 2022). miR-224-5p has been confirmed a tumor promoter in various malignant tumors, for instance, papillary thyroid carcinoma, colorectal cancer, and non-small cell lung cancer (Zang *et al.*, 2020, Zhou *et al.*, 2021, Wu *et al.*, 2022). As unraveled in this work, miR-224-5p was expressed excessively in HCC tissues and cells and the HCC patients with miR-224-5p

expressed highly possessed a poor survival rate; LYC could diminish the miR-224-5p content, inhibiting the HCC advance promoted by over-expressed miR-224-5p. EMT is such a course in which polarized epithelial cells become in-adhesive, transforming into a phenotype of mesenchymal cell (Chen *et al.*, 2017). EMT is linked to tumor development as it can boost cell movement and penetration and resist apoptosis stimuli, bestowing metastatic properties on cancer cells; in turn, the metastasis of cancer cells is a major cause of death from cancer (Mittal, 2018). EMT is typically featured by reduced E-cadherin contents and elevated contents of vimentin, N-cadherin, snail, and the like proteins of mesenchymal markers (Pallasch *et al.*, 2020, Xu *et al.*, 2023). Through this survey, a sharp reduction in E-cadherin contents and a great rise in N-cadherin contents were detected in HCC cells following the excessive expression of miR-224-5p. This consequence reveals that the excessively-expressed miR-224-5p contributed to EMT, which however was suppressed after LYC administration.

With such mechanisms as promoting inflammation, the tumor immune microenvironment is important for cancer development (Oura *et al.*, 2021). IFN-γ, a regulator crucial in mediating immune responses in cells, functions in promoting immune regulation and resisting viruses and cancers (Jorgovanovic *et al.*, 2020, Ding *et al.*, 2022). The function of immune cells and the immune balance in local tissues can be affected directly by the activity of IL-2, a core factor involving in immune response and regulation (Abbas *et al.*, 2018, Bae *et al.*, 2022). TNF-α and IL-1β are both pro-inflammatory cytokines, where the former is primarily secreted by tumor-associated macrophages and cancer cells (Cruceriu *et al.*, 2020) while the latter involves in many rheumatic and inflammatory diseases and contributes to tumor progression (Han *et al.*, 2023). As uncovered in this survey, miR-224-5p, when expressed excessively, depressed the expressions of IFN-γ and IL-2 in cells (MHCC97 and SMMC-7721) and heightened those of TNF-α and IL-1β to a large extent; whereas, this phenomenon was offset with the administration of LYC. This finding proves that miR-224-5p over expression could enhance inflammatory responses in HCC while LYC could refrain such responses.

For further expounding the actions of miR-224-5p in controlling the malignant advance of HCC, GEPIA and Target Scan Human databases were searched and assessed. Ultimately, COLEC10 was judged as a target gene located in the downstream of miR-224-5p. This gene is a C-type lectin primarily existing in the liver and can take part in HCC advance (Cai *et al.*, 2023). COLEC10's targeting relationship with miR-224-5p was verified through Dual-Luciferase reporter assays in this survey. Consequently, the activity, movement and penetration abilities of HCC cells inhibited by silencing miR-224-5p

was somewhat offset following the silencing of COLEC10. This data prove that miR-224-5p could attenuate the expression of COLEC10 in a targeted way. Besides, the in vivo experiment revealed that the dosing of LYC led to a remarkable decline in miR-224-5p levels and a great increment in COLEC10 levels. Hence, LYC depressed HCC worsening by dampening the miR-224-5p/COLEC10 axis.

CONCLUSION

In brief, miR-224-5p was over-expressed significantly in HCC tissues and cells; by negatively adjusting the COLEC10 level, miR-224-5p exacerbated HCC. Following the dosing of LYC, the miR-224-5p expression was restrained, holding up the exacerbation of HCC. Therefore, miR-224-5p and COLEC10 can serve as new biomarkers. The potential of LYC in treating HCC lays a fresh theoretical foundation for the diagnosis and intervention of HCC in the early stage. However, this study still has some limitations, and the safety of LYC in *vivo* needs further evaluation.

REFERENCES

Abbas AK, Trotta EDRS, Marson A and Bluestone JA (2018). Revisiting IL-2: Biology and therapeutic prospects. *Science Immunology,* **3**(25): eaat1482.

Alkreathy HM and Esmat A (2022). Lycorine ameliorates thioacetamide-induced hepatic fibrosis in rats: Emphasis on antioxidant, anti-inflammatory, and STAT3 inhibition effects. *Pharmaceuticals (Basel),* **15**(3): 369.

Ayuso C, Rimola J, Vilana R, Burrel M, Darnell A, García-Criado Á, Bianchi L, Belmonte E, Caparroz C, Barrufet M, Bruix J and Bru C (2018). Diagnosis and staging of hepatocellular carcinoma (HCC): Current guidelines. *Eur. J. Radiol.,* **101**: 72-81.

Bae J, Liu L, Moore C, Hsu E, Zhang A, Ren Z, Sun Z, Wang X, Zhu J, Shen J, Qiao J and Fu YX (2022). IL-2 delivery by engineered mesenchymal stem cells re-invigorates CD8^{+} T cells to overcome immunotherapy resistance in cancer. *Nat. Cell Biol.,* **24**(12): 1754-1765.

Cai MN, Chen DM, Xiao LX, Li SS, Liao CH, Li J, Huang ZX, Wang JL, Gu YR, Gu L, Huang YH and Lian YF (2023). COLEC10 induces endoplasmic reticulum stress by occupying GRP78 and inhibits hepatocellular carcinoma. *Lab. Invest,* **103**(7): 100130.

Chedid MF, Kruel CRP, Pinto MA, Grezzana-Filho TJM, Leipnitz I, Kruel CDP, Scaffaro LA and Chedid AD (2017). Hepatocellular carcinoma: Diagnosis and operative management. *Arquivos brasileiros de cirurgia digestiva: ABCD = Brazilian archives of digestive surgery,* **30**(4): 272-278.

Chen T, You Y, Jiang H and Wang ZZ (2017). Epithelial-mesenchymal transition (EMT): A biological process

in the development, stem cell differentiation and tumorigenesis. *J. Cell Physiol.,* **232**(12): 3261-3272.

Cruceriu D, Baldasici O, Balacescu O and Berindan-Neagoe I (2020). The dual role of tumor necrosis factor-alpha (TNF-α) in breast cancer: Molecular insights and therapeutic approaches. *Cell Oncol. (Dordr.)* **43**(1): 1-18.

Di Sotto A, Valipour M, Azari A, Di Giacomo S and Irannejad H (2023). Benzoindolizidine alkaloids tylophorine and lycorine and their analogues with antiviral, anti-inflammatory, and anticancer properties: Promises and challenges. *Biomedicines* **11**(10): 2619.

Diener C, Keller A and Meese E (2022). Emerging concepts of miRNA therapeutics: From cells to clinic. *Trends Genet.,* **38**(6): 613-626.

Ding H, Wang G, Yu Z, Sun H and Wang L (2022). Role of interferon-gamma (IFN-γ) and IFN-γ receptor 1/2 (IFNγR1/2) in regulation of immunity, infection, and cancer development: IFN-γ-dependent or independent pathway. *Biomed. Pharmacother.,* **155**: 113683.

Foglia B, Turato C and Cannito S (2023). Hepatocellular carcinoma: Latest research in pathogenesis, detection and treatment. *Int. J. Mol. Sci.* **24**(15): 12224.

Han Y, Zhang YY, Pan YQ, Zheng XJ, Liao K, Mo HY, Sheng H, Wu QN, Liu ZX, Zeng ZL, Yang W, Yuan S Q, Huang P, Ju HQ and Xu RH (2023). IL-1β-associated NNT acetylation orchestrates iron-sulfur cluster maintenance and cancer immunotherapy resistance. *Mol. Cell,* **83**(11): 1887-1902.e1888.

Hartke J, Johnson M and Ghabril M (2017). The diagnosis and treatment of hepatocellular carcinoma. *Semin. Diagn. Pathol.,* **34**(2): 153-159.

Hassanipour S, Vali M, Gaffari-Fam S, Nikbakht HA, Abdzadeh E, Joukar F, Pourshams A, Shafaghi A, Malakoutikhah M, Arab-Zozani M, Salehiniya H and Mansour-Ghanaei F (2020). The survival rate of hepatocellular carcinoma in Asian countries: A systematic review and meta-analysis. *EXCLI Journal,* **19**: 108-130.

He B, Zhao Z, Cai Q, Zhang Y, Zhang P, Shi S, Xie H, Peng X, Yin W, Tao Y and Wang X (2020). miRNA-based biomarkers, therapies and resistance in Cancer. *Int J Biol Sci.,* **16**(14): 2628-2647.

Hu M, Yu Z, Mei P, Li J, Luo D, Zhang H, Zhou M, Liang F and Chen R (2020). Lycorine Induces autophagy-associated apoptosis by targeting MEK2 and enhances vemurafenib activity in colorectal cancer. *Aging (Albany N. Y.)* **12**(1): 138-155.

Hu Z, Zhao Y, Mang Y, Zhu J, Yu L, Li L and Ran J (2023). MiR-21-5p promotes sorafenib resistance and hepatocellular carcinoma progression by regulating SIRT7 ubiquitination through USP24. *Life Sciences,* **325**: 121773.

Jorgovanovic D, Song M, Wang L and Zhang Y (2020). Roles of IFN-γ in tumor progression and regression: A review. *Biomarker research,* **8**: 49.

Li D, Zhang J and Li J (2020). Role of miRNA sponges in hepatocellular carcinoma. *Clin. Chim. Acta.,* **500**: 10-19.

Li Y and Jiang A (2020). ST8SIA6-AS1 promotes hepatocellular carcinoma by absorbing miR-5195-3p to regulate HOXB6. *Cancer Biol Ther.,* **21**: 647-655.

Li Z, Zhou Q, Liu X, Li Y, Fan X and Liu G (2022). Lycorine upregulates the expression of RMB10, promotes apoptosis and inhibits the proliferation and migration of cervical cancer cells. *Int. J. Mol. Med.* **50**(6): 145.

Li Z, Wu L, Tan W, Zhang K, Lin Q, Zhu J, Tu C, Lv X and Jiang C (2021). MiR-20b-5p promotes hepatocellular carcinoma cell proliferation, migration and invasion by down-regulating CPEB3. *Ann Hepatol.* **23**: 100345.

Mittal V (2018). Epithelial mesenchymal transition in tumor metastasis. *Annu. Rev. Pathol.,* **13**: 395-412.

Nagaraju GP, Dariya B, Kasa P, Peela S and El-Rayes BF (2022). Epigenetics in hepatocellular carcinoma. *Semin. Cancer Biol.,* **86**(Pt 3): 622-632.

Oura K, Morishita A and Masaki T (2020). Molecular and functional roles of MicroRNAs in the progression of hepatocellular carcinoma - A review. *Int. J. Mol. Sci.* **21**(21): 8362.

Oura K, Morishita A, Tani J and Masaki T (2021). Tumor immune microenvironment and immunosuppressive therapy in hepatocellular carcinoma: A review. *Int. J. Mol. Sci.,* **22**(11): 5801.

Pallasch FB and Schumacher U (2020). Angiotensin inhibition, TGF-β and EMT in cancer. *Cancers (Basel).,* **12**(10): 2785.

Roy M, Liang L, Xiao X, Feng P, Ye M and Liu J (2018). Lycorine: A prospective natural lead for anticancer drug discovery. *Biomed. Pharmacother.,* **107**: 615-624.

Sartorius K, Sartorius B, Winkler C, Chuturgoon A and Makarova J (2018). The biological and diagnostic role of miRNA's in hepatocellular carcinoma. *Frontiers in bioscience (Landmark edition),* **23**(9): 1701-1720.

Shen J, Zhang T, Cheng Z, Zhu N, Wang H, Lin L, Wang Z, Yi H and Hu M (2018). Lycorine inhibits glioblastoma multiforme growth through EGFR suppression. *J. Exp. Clin. Cancer Res.,* **37**(1): 157.

Sun Y, Gu Y, Gao X, Jin X, Wink M, Sharopov FS, Yang L and Sethi G (2023). Lycorine suppresses the malignancy of breast carcinoma by modulating epithelial mesenchymal transition and β-catenin signaling. *Pharmacol. Res.,* **195**: 106866.

Wang F, Xie Z, Zhang N, Ding H, Xiong K, Guo L, Huang H and Wen Z (2022). Has_circ_0008583 modulates hepatocellular carcinoma progression through the miR-1301-3p/METTL3 pathway. *Bioengineered.,* **13**: 1185-1197.

Wang N, Li P, Liu J and Wang Z (2023). MiR-29a-3p promotes nasal epithelial barrier dysfunction via direct targeting of CTNNB1-VCL module in allergic rhinitis. *Int. Immunopharmacol.,* **120**: 110325.

Wang Y, Wang P, Zhao L, Chen X, Lin Z, Zhang L and Li Z (2021). miR-224-5p Carried by Human Umbilical Cord Mesenchymal Stem Cells-Derived Exosomes Regulates Autophagy in Breast Cancer Cells via HOXA5. *Front Cell Dev Biol.*, **9**: 679185.

Wen NY, Cai YL, Li FY, Ye H, Tang W, Song PP and Cheng NS (2022). The clinical management of hepatocellular carcinoma worldwide: A concise review and comparison of current guidelines: 2022 update. *Biosci. Trends* **16**(1): 20-30.

Wu F, Yang J, Shang G, Zhang Z, Niu S, Liu Y, Liu H, Jing J and Fang Y (2022). Exosomal miR-224-5p from colorectal cancer cells promotes malignant transformation of human normal colon epithelial cells by promoting cell proliferation through downregulation of CMTM4. *Oxid. Med. Cell. Longev.* 5983629.

Xu J, Wang Y, Jiang J, Yin C and Shi B (2023). ADAM12 promotes clear cell renal cell carcinoma progression and triggers EMT via EGFR/ERK signaling pathway. *J. Transl. Med.,* **21**(1): 56.

Yu H, Qiu Y, Pang X, Li J, Wu S, Yin S, Han L, Zhang Y, Jin C, Gao X, Hu W and Wang T (2017). Lycorine promotes autophagy and apoptosis via TCRP1/Akt/mTOR axis inactivation in human hepatocellular carcinoma. *Mol. Cancer Ther.* **16**(12): 2711-2723.

Zang CS, Huang HT, Qiu J, Sun J, Ge RF and Jiang LW (2020). MiR-224-5p targets EGR2 to promote the development of papillary thyroid carcinoma. *Eur. Rev. Med. Pharmacol. Sci.,* **24**(9): 4890-4900.

Zhai J, Jiang JF and Shi L (2023). Lycorine weakens tamoxifen resistance of breast cancer via abrogating HAGLR-mediated epigenetic suppression on VGLL4 by DNMT1. *Kaohsiung J Med Sci.*, **39**: 278-289.

Zhang L, Huang L, Liang H, Zhang R, Chen G, Pang Y and Feng Z (2017). Clinical value and potential targets of miR-224-5p in hepatocellular carcinoma validated by a TCGA- and GEO- based study. *Int. J. Clin. Exp. Pathol.,* **10**(9): 9970-9989.

Zhou J, Wang H, Sun Q, Liu X, Wu Z, Wang X, Fang W and Ma Z (2021). miR-224-5p-enriched exosomes promote tumorigenesis by directly targeting androgen receptor in non-small cell lung cancer. *Mol. Ther. Nucleic Acids,* **23**: 1217-1228.